

PRODUCTION TESTS, CALIBRATIONS, AND COMMISSIONING OF BUTTON BPMS FOR THE EUROPEAN XFEL*

D.M. Treyer, B. Keil, W. Koprek, PSI, Villigen, Switzerland
 D. Lipka, DESY, Hamburg, Germany

Abstract

Commissioning of the entire European XFEL started early 2017. More than 300 button-electrode type beam position monitors (BPMS) are used in its cold Linac and warm beam transfer lines. Signal processing in the BPM RF front-end (RFFE) electronics employs signal stretching by chirp filtering, switchable gain stages, digital step attenuators, and peak detection. In this paper we present details on RF front-end production tests, calibration, and BPM beam commissioning results. Furthermore, a calibration pulser circuit that is built into each BPM electronics is presented. The setup and algorithms for production calibration of all RFFEs are described. Finally, resolution measurements obtained by correlation among all XFEL BPMS (including cavity and re-entrant types) are presented, confirming that the system can be used for orbit correction and transmission measurement down to bunch charges of a few pico-Coulombs.

INTRODUCTION

The European XFEL (E-XFEL) is a free electron laser with a 17.5 GeV superconducting linac and currently five experimental end stations with three undulators for producing trains of (sub-)fs-duration X-ray pulses with a wavelength range down to 0.1 nm. The accelerator works in train-pulsed mode at 10 Hz repetition rate. Up to 2700 bunches with a bunch spacing down to 222 ns can be produced in a single train. The accelerator is built in underground tunnels of >5 km total length. It is equipped with ~460 BPM pickups of five types: warm and cold buttons [1], cold re-entrant cavities, and warm dual-resonator cavities with two aperture sizes. More than 304 BPMS use cold and warm button pickups. The E-XFEL is an international project where Switzerland provides electronics for all electron BPMS [2] except 24 re-entrant BPM RFFEs, as well as the transverse intra-train beam based feedback system (IBFB) [3] as in-kind contributions. Production and commissioning of this comparatively large amount of BPM electronics motivated an automated production test system. The tasks of this test system include quality checks of the produced electronic boards, calibration and performance verification of complete BPM electronics, and documentation of test results as a part of the deliverables.

BUTTON BPM ELECTRONICS OVERVIEW

Electronics for up to four button BPMS (four channels each) are housed in a modular BPM unit (MBU), a cus-

tomized crate that can be used for different types of BPMS [4]. On the rear side it has slots for modular power supply and interface boards. On the front side it has slots for a digital carrier board (GPAC) with two analog-to-digital converter (ADC) mezzanine boards, and up to four button BPM RF front ends (RFFEs). Mixed configurations consisting of button, cavity, and/or re-entrant type BPMS are also possible.

The task of the RFFEs is to condition the signals from the beam pickups for digitization by the ADCs. Figure 1 shows the block diagram of the button BPM type RFFE [5]. One out of four identical channels is shown. In summary, the RFFE electronics first stretches the very short incoming pickup signal pulse by a dispersive chirp filter, then amplifies/attenuates the stretched signal, and finally detects its amplitude by diode based peak detectors. An onboard pulser can generate pickup-like signals for beam emulation, self-testing, and calibration purposes. Switches at the RF inputs allow selection of the beam pickup or the on-board pulser signal.

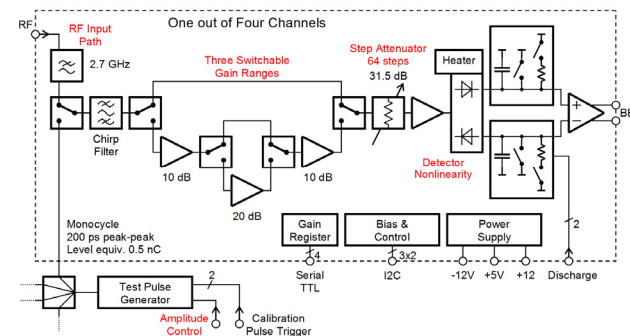


Figure 1: Block diagram of a single RFFE channel. Red labeled items need calibration.

CALIBRATION PULSER

The purpose of the onboard calibration pulser is to enable RFFE built-in test and calibration without the need for an external test signal source. The pulser should therefore ideally provide a signal having waveform, spectrum, and repetition rate matching the typical E-XFEL button pickup. An earlier design based on an avalanche transistor was later superseded by a design based on a step-recovery diode (SRD). This resulted in higher repetition rate (5 MHz), excellent pulse amplitude stability (1% rms), much better spectral matching to the pickup signal (peak at 2 GHz), and the ability to adjust the pulse amplitude (≈ 8 Vpp max.) over a wide range (26 dB).

Figure 2 shows the pulser block diagram. After the trigger rising edge, the SRD is forward biased during roughly 50 ns. Then the current is reversed and boosted

*Work supported by Swiss State Secretariat for Education, Research and Innovation.

Content from this work may be used under the terms of the CC BY 3.0 licence (© 2018). Any distribution of this work must maintain attribution to the author(s), title of the work, publisher, and DOI.

by roughly a factor of five over a transition time of <2 ns. After a few nanoseconds, the SRD snaps, thereby producing a very abrupt current edge with a transition time of <150 ps. This edge is converted to a monocycle pulse by the pulse shaping networks. Keeping the ratio of the adjustable SRD forward to reverse currents constant reduces the parasitic dependence of trigger latency on amplitude. See Fig. 3 for the resulting output waveform and amplitude control characteristics.

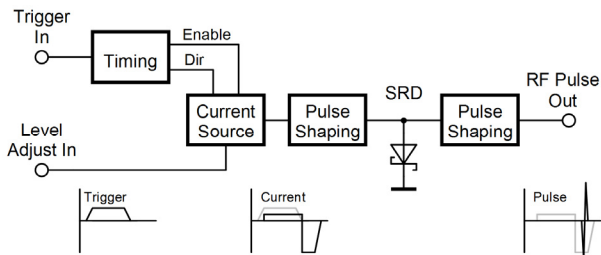


Figure 2: Block diagram of the pulser circuit.

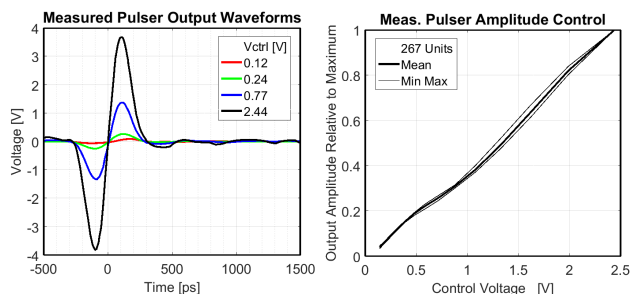


Figure 3: Exemplary measured pulser output waveform (left), and amplitude control characteristic (right).

PRODUCTION TESTS

PSI delivered fully tested and calibrated BPM electronics to E-XFEL, thus allowing to reliably measure beam position and transmission at first beam. This required not only functional tests of RF/analog and digital electronics, but also calibration of the RF/analog signal paths. To achieve this, the following test and calibration sequence was applied:

1. MBU crate and GPAC digital carrier board test
2. ADC tests
3. Pre-calibration RFFE functional test
4. RFFE calibration with onboard pulser
5. RFFE calibration and test with external pulser
6. Burn-in test of complete BPM electronics

The test setup used two 19" racks where a total of 16 MBUs could be tested. This allowed running automated calibrations on MBUs in one rack, while setting up MBUs and performing pre-calibration tests in the other rack.

The calibration with the onboard pulser takes half an hour per RFFE, and was done in parallel on several RFFEs. In contrast, the RFFE calibration with external pulser requires the test operator to connect RF cables and thus is time consuming. Two external pulsers developed at

PSI were used, allowing to perform this calibration simultaneously on two MBUs.

All tests and calibrations were automated by Matlab scripts. Comprehensive test reports were generated for individual components (MBU, GPAC, ADC, and RFFE), as well as for each complete BPM electronics unit.

PRODUCTION CALIBRATION OF EACH RF FRONT-END ELECTRONICS

This section describes the theory and algorithms used for the previously mentioned RFFE calibration with onboard pulser and RFFE calibration with external pulser.

Detector Linearization

Since the amplitude detectors are based on diodes, they exhibit a nonlinear transfer characteristic. To achieve minimal charge-dependence of measured beam position, the nonlinearity must be accounted for. During operation, this is achieved by applying an inverse nonlinear function to the measured pulse heights in the FPGA-based digital post-processing. During production time, the nonlinearity was measured and fitted to a suitable model.

Exemplary transfer functions are shown in Fig. 4 (black). They were measured by using the RFFE onboard pulser and varying the digital step attenuator (in the lowest of the three gain ranges) to generate an amplitude sweep of the detector input signal, while the detector output voltage (pulse height) was measured by the ADC.

Note that due to unavoidable production tolerances of the electronic components and slight differences in the component layout of the four channels, each channel of each RFFE has to be calibrated individually. This is the case not just for the detector linearization but for all applied calibration procedures.

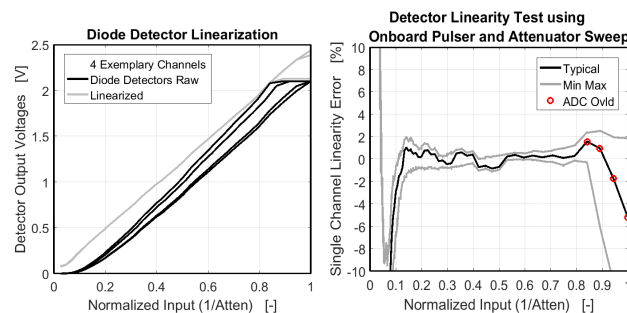


Figure 4: Detector linearization (left), and linearization residual error (right) of ≈ 300 units.

A suitable approximation for the detector nonlinear transfer function is:

$$y = \sqrt[c]{a^c + (bx)^c} - a \quad (1)$$

Here y is the detector output voltage measured by the ADC (pulse height), and x is the detector RF input voltage amplitude. Parameter a is an offset in x , parameter b is a gain (detector sensitivity and RF chain), and parameter c is the curvature at the threshold of the detector. The threshold itself is at $x = a/b$, and becomes more pro-

nounced (edged) as c is increased. This approximation describes the asymptotic behaviour of the detector correctly, and does have an inverse.

The linearized detector characteristics are also shown in Fig. 4 (grey). Good linearity is achieved for normalized input signals ranging from 0.15 to 0.85, where the lower limit is determined by the diode detector threshold, and the upper limit by the ADC saturation level. This is illustrated by the graph on the right, which shows the relative deviation from an exactly linear transfer function.

The linearity of the RFFE is calibrated before the calibration of the step attenuators. However, by using many attenuator steps, and due to the limited degrees of freedom of the detector transfer function approximation, the effects of step attenuator errors are averaged out. This method provides absolute levels for detector output voltage y , where the precision is mainly determined by the ADC and its voltage reference.

Gain Range and Step Attenuator Calibration

When the gain range or digital step attenuator settings are changed while the beam orbit remains constant, the measured beam position should remain unchanged. This requires precise knowledge of gain and attenuation values of the three gain ranges and the digital step attenuator for each channel. Because of electronics component tolerances and the effects of internal signal reflections, the gain ranges and digital step attenuators need to be calibrated to achieve the desired performance.

The applied calibration procedure utilizes the onboard pulser and the (already calibrated) detectors to measure the effects of different gain range and step attenuator settings. The dependence of detected signal level D on pulser amplitude P , gain range G and step attenuator A is given by the following equation:

$$P_p + G_g^i - A_a^i = D_{p,g,a}^i \quad (2)$$

Here P_p is the p -th pulser amplitude in [dBm], G_g is the gain value in [dB] of the g -th gain range, A_a is the attenuation value in [dB] of the a -th attenuator step, and $D_{p,g,a}^i$ is the resulting detected signal level in [dBm]. Index i is the channel number. Equation (2) can be written as a linear system of equations and solved for P_p , G_g , and A_a , given that measurements are available at sufficient combinations of p , g , and a . Since P , G , and A are not independent, two constraints are added: The *measured* mean attenuator value is forced to equal the *nominal* mean attenuator value for every channel; and the mean measured gain at lowest gain is forced to zero:

$$\sum_a A_a^i - A_{a,nom}^i = 0 \quad \text{and} \quad \sum_i G_1^i = 0 \quad (3)$$

Calibration results are shown in Fig. 5 in the form of deviations of attenuation and gain values from their nominal values. The measured G_g^i and A_a^i are saved to the RFFE's EEPROM, and later used by the FPGA board for position and charge calculations.

The deviation of measured gain from its nominal value increases for higher gain ranges, because more amplifier stages are involved. This calibration also yields the measured pulser amplitude P_p vs. pulser control voltage characteristics, as shown in Fig. 3.

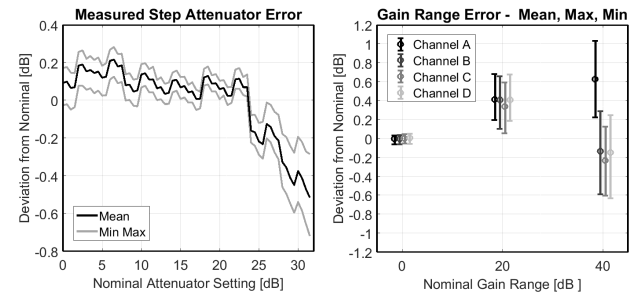


Figure 5: Calibration results from step attenuators (left) and gain ranges (right) for ≈ 300 units.

RFFE Calibration with External Pulser

The signal paths from the RF inputs to the RF switches (see block diagram) cannot be tested (for defects) and calibrated by means of the onboard pulser. Also, the onboard pulser is not an absolute amplitude reference. A known signal must therefore be applied to obtain gain correction factors for the four RF inputs and for absolute charge calibration. For this purpose, two button pickup signal generators (BPSGs) with four output channels each have been built, carefully characterized, and utilized.

The BPSGs are also used to verify the gain range and step attenuator calibration previously performed with the onboard pulser. Residual beam position and charge measurement errors caused by the limitations of the calibration are shown in Fig. 6. For the typical units shown, the multiple marks seen at every attenuator setting correspond to measurements taken at different signal levels. The spread is caused by residual detector linearity errors and pulser signal level errors (the latter affecting charge only).

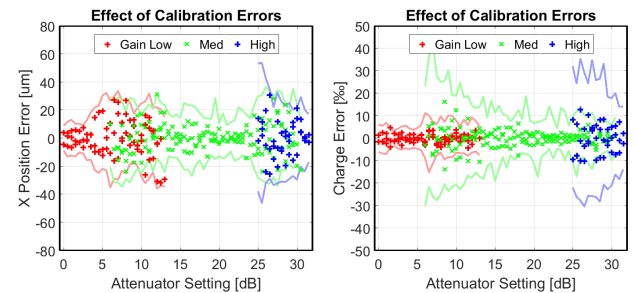


Figure 6: Effect of calibration errors on measured beam position and charge for a typical RFFE (crosses) and ≈ 50 RFFEs (solid lines).

BURN-IN TEST

The very last step of the production process was the burn-in test, typically running over several days, to verify reliable operation of the fully assembled, ready-to-ship BPM systems. During burn-in, the onboard pulser was emulating the BPM pickup signal of an electron beam running at 10 Hz repetition rate.

Content from this work may be used under the terms of the CC BY 3.0 licence (© 2018). Any distribution of this work must maintain attribution to the author(s), title of the work, publisher, and DOI.

The FPGAs processing the BPM data have an on-chip microprocessor that reads the measured charge and position values from the FPGAs, and performs continuous real-time calculations of statistical quantities such as average values, standard deviations, and peak-peak variations. These quantities were collected and observed by external test software (Matlab script) through each MBU's Ethernet interface, and used as acceptance criteria for the burn-in test, by detecting MBUs where the peak-peak values were outside the acceptance range.

Since each RFFE has its own onboard pulser and each pair of BPMs shares one embedded processor, burn-in tests of all BPMs could be performed in parallel for a large number of MBUs before shipment. During the burn-in tests, units were also switched off and on several times, to introduce thermal stress, and to verify that they were fully functional after each power cycle.

RESOLUTION MEASUREMENTS AT EUROPEAN XFEL

First position and charge resolution measurements of button, re-entrant, and cavity type BPMs in the E-XFEL injector have already been presented earlier [6] for a fixed bunch charge of 400 pC. Figure 7 shows mean values of measured single-bunch position and charge resolutions of BPMs in the E-XFEL linac as a function of bunch charge.

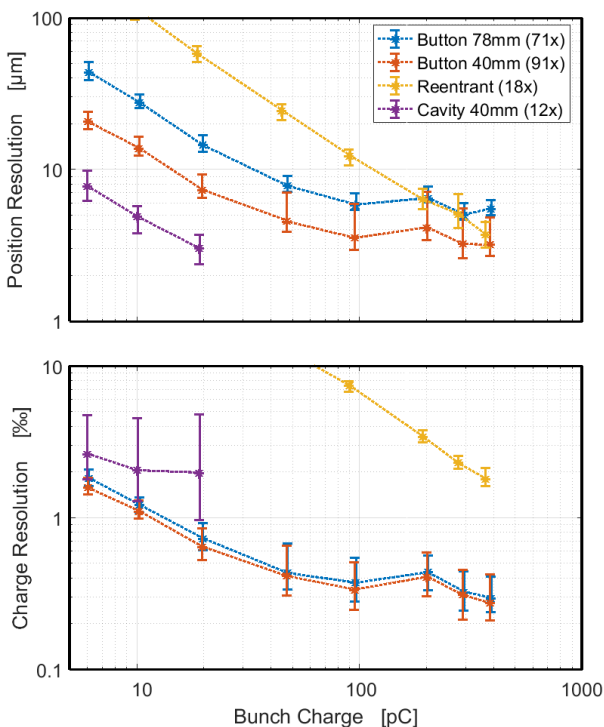


Figure 7: Measured BPM single-bunch resolutions.

The numbers of BPMs used for the statistics (mean values and $\pm 1\sigma$ bars) are indicated in the legend (bracket values). Measured single-bunch position and charge resolution values are also shown in Table 1 for 20 pC and 100 pC bunch charges.

It should be noted that the measured resolutions (rms random noise) may have been degraded by systematic measurement errors resulting from changes of RFFE attenuator and gain range settings by the action of the automatic gain control algorithms in the FPGAs. The presented resolution measurements are based on correlation analysis among all BPMs along the machine [7].

Table 1: Measured BPM Single-bunch Resolutions

BPM Type	Position Resolution [μm]		Relative Charge Resolution [%]	
	20 pC	100 pC	20 pC	100 pC
Cold Buttons	15	6	0.75	0.4
Warm Buttons	8	4	0.65	0.4

CONCLUSIONS

Electronics for more than 300 button-electrode type BPM systems were produced, calibrated and delivered to the European XFEL. So far about 240 systems were installed in the E-XFEL tunnel and have been delivering charge and position measurements since first beam in beginning of 2017. Only one RFFE board had to be replaced shortly after installation due to hardware failure, which proves the effectiveness of the quality checks. The electronics work very reliably, and the resolutions measured with beam show that the requirement (e.g. $<50 \mu\text{m}$ for single-bunch position at 100 to 1000 pC) are not only achieved, but significantly exceeded by a factor of almost ten. This allows to operate the E-XFEL at very low bunch charges, and to characterize the accelerator more accurately at higher bunch charges. The reported resolutions were achieved with electronics calibrated in the laboratory only. Remaining systematic errors could be further reduced by beam-based calibration methods in the future.

REFERENCES

- [1] D. Lipka *et al.*, "Button BPM development for the European XFEL", in *Proc. DIPAC'11*, Hamburg, Germany, 2011, pp. 83-85.
- [2] B. Keil *et al.*, "The European XFEL beam position monitor system", in *Proc. IPAC'10*, Kyoto, Japan, 2010, pp. 1125-1127.
- [3] W. Koprek *et al.*, "Status of the transverse intra-bunch train feedback of the European XFEL", presented at IBIC'17, Grand Rapids, MI, USA, paper TU3AB2, this conference.
- [4] B. Keil *et al.*, "A generic BPM electronics platform for European XFEL, SwissFEL and SLS", in *Proc. IBIC'12*, Tsukuba, Japan, 2012, pp 133-137.
- [5] D.M. Treyer *et al.*, "Design and beam test results of button BPMs for the European XFEL", in *Proc. IBIC'13*, Oxford, UK, 2013, pp. 723-726.
- [6] D. Lipka *et al.*, "First experience with the standard diagnostics at the European XFEL injector", in *Proc. IBIC'16*, Barcelona, Spain, 2016, pp.14-19.
- [7] N. Baboi *et al.*, "Resolution studies at beam position monitors at the FLASH facility at DESY", in *Proc. BIW'06*, Fermilab, Batavia, Illinois, USA, 2006, in *Proc. AIP Conf. vol. 868*, Ed. T.S. Meyer, R.C. Webber, pp. 227-237.